Processing biomedical signals

Giuseppe Nardulli
Physics Dept. and Center TIRES
University of Bari, Italy

Synchronization

- Periodic physiological signals (e.g. circadian rithms, arterial pressure, α rithms in EEG, and many more) : cooperative phenomena due to a large number of self-organizing microscopic coupled oscillators.
- Synchronization result of coupling and anharmonicity (non-linearity)

I pendoli di Huygens

Il problema della longitudine nel 1600 e la Royal Society
Soluzione astronomica (Galileo e le eclissi dei satelliti di Giove)
e la soluzione degli orologiai.

- Ma gli orologi dovevano essere sincronizzati. Huygens nel 1665:
  Essendo obbligato a rimanere nella mia stanza mi tenevo occupato nel fare osservazioni su miei due nuovi orologi. Ho notato un effetto meraviglioso che nessuno avrebbe mai immaginato. Questi due orologi, posti alla distanza di uno o due piedi raggiungono un accordo così esatto da oscillare insieme senza alcuna variazione. Sono giunto alla conclusione che questo avviene per una sorta di simpatia. Dopo esser stati disordinati i due pendoli tornano alla consonanza dopo circa mezz'ora e restano poi sincronizzati per tutto il tempo che si vuole. Li ho separati fino alla distanza di 15 piedi: dopo un giorno ritardavano di 5 secondi: credo che il loro accordo precedente sia dovuto ad una impercettibile agitazione dell'aria dovuta al loro moto.

S. Strogatz, Sync

Synchronized flashing of fireflies

- Discovered first in Malaysia: colonies of thousands fireflies flashing
- Flashing is used to guide courtship In groups.
- Flashing rapidly becomes highly synchronized (only males)

Explanations

- Accidental ?
- Observers's blinking of eyes ?
- Puffs of winds ?

- Actually fireflies have neural timing mechanism, i.e. an oscillator that is stimulated by flashing light

Human behavior can be similar

- Finger tapping:
- Close your eyes and tap fingers: almost immediately the two movements become synchronous

Synchronization in brain

- N. Wiener and the α waves: in the early ’50 he was studying EEG (first introduced in 1929) and the prominent α band **(7.5-12.5 Hz)**; assumed that neurons participating to that band, taken individually, would spike periodically with different frequencies. Taken together they form a clock with an average frequency of ca. 10 beats each second

Wiener, the α waves and beyond

EEG rithms:

δ(0.5-3.5 Hz):deep sleep

θ(3.5-7.5 Hz):sleep

α(7.5-12.5 Hz): wake,relax

β (12.5-30 Hz): tension

γ (30-60 Hz): Cellular level exp.

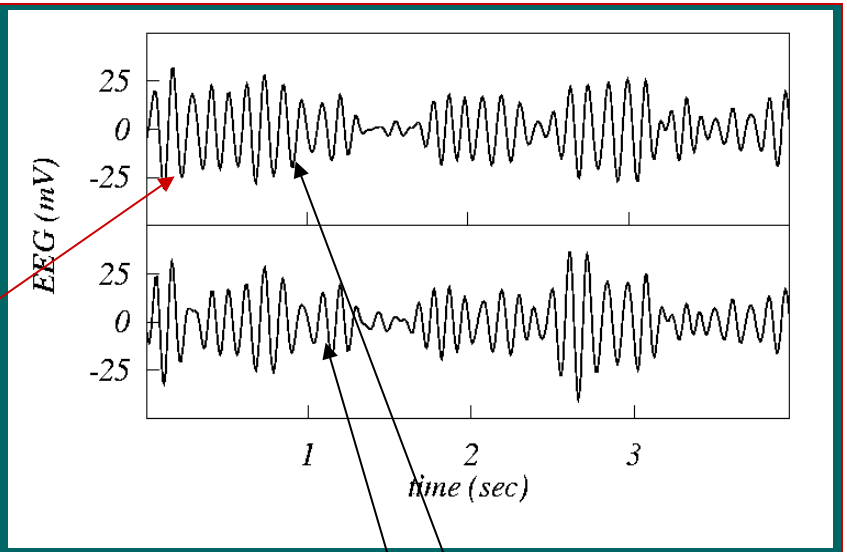

Periodicity is produced by spontaneous synchronization of microscopic signals

Synchronization between signals from different electrodes can be noted,

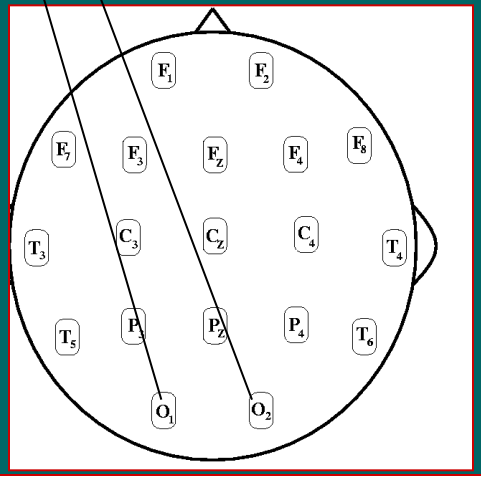

Can synchronization be used for diagnostic purposes?

EEG synchronization and migraine

(L. Angelini et al. TIRES Center and Boston Univ. PRL, 2004)

- Migraine: an incapacitating disorder of neurovascular origin. It consists of attacks of headache, accompanied by various neurological symptoms. In the US 5% of people suffer at least 18 days of migraine per year (more than 1% have at least one day of migraine a week).
- No experimental model fully explains the migraine process. A wide range of events can alter conditions in the brain and trigger migraines.

How the response of migraine patients to such events differs from that of healthy persons?

Data set consists of EEG taken in the laboratories of the Neurophysiology Dept. at University of Bari

Measuring synchronization:

Method of the phase synchronization (study of synchronization of the phases, not the signals themselves):

$$y(t) = \frac{1}{\pi} P.V. \int_{-\infty}^{+\infty} \frac{x(\tau)}{t-\tau} d\tau$$

Analytic signal $z(t) = x(t) + iy(t) = A(t)e^{i\phi(t)}$

Hilbert Transform

For each Fourier component:

$$S(t) = A \cos \omega t$$

$$H.T.\{ S\} = A \sin \omega t$$

Analogous to dispersion relations

Generalized phase difference

$$\Phi_{n,m}(t) = \left[m\varphi_1(t) - n\varphi_2(t) \right]_{\mathrm{mod}\, 2\pi}$$

Here n=m=1; other choices don't lead to interesting results

T3-T5 pair of electrodes

a) Healthy patient without stimulus
b) Same with 9Hz flash
c) Patient without stimulus
d) Same with stimulus

Data filtered in the α band

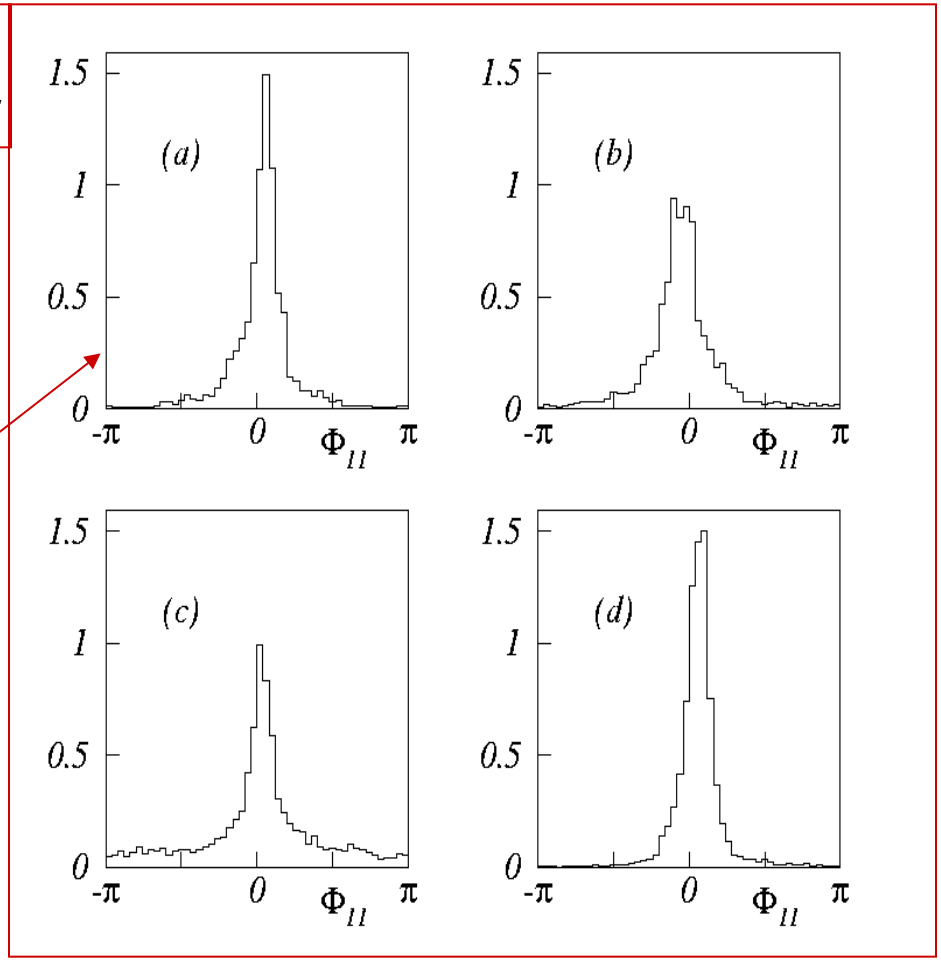

Discriminating controls and patients:
synchronization increases for patients, with a stimulus

$\Gamma = \text{Log } \rho^f / \rho^{sp}$

$\rho = 1 - S / S_{max}$

S = Shannon entropy for the $\Phi_{1,1}$ histogram;
S_{max} = maximal entropy (uniform distribution)

ρ^f : with flash
ρ^{sp} : spontaneous

Γ represented for all electrodes; averaged over electrodes and over patients/controls; 24 Hz flash

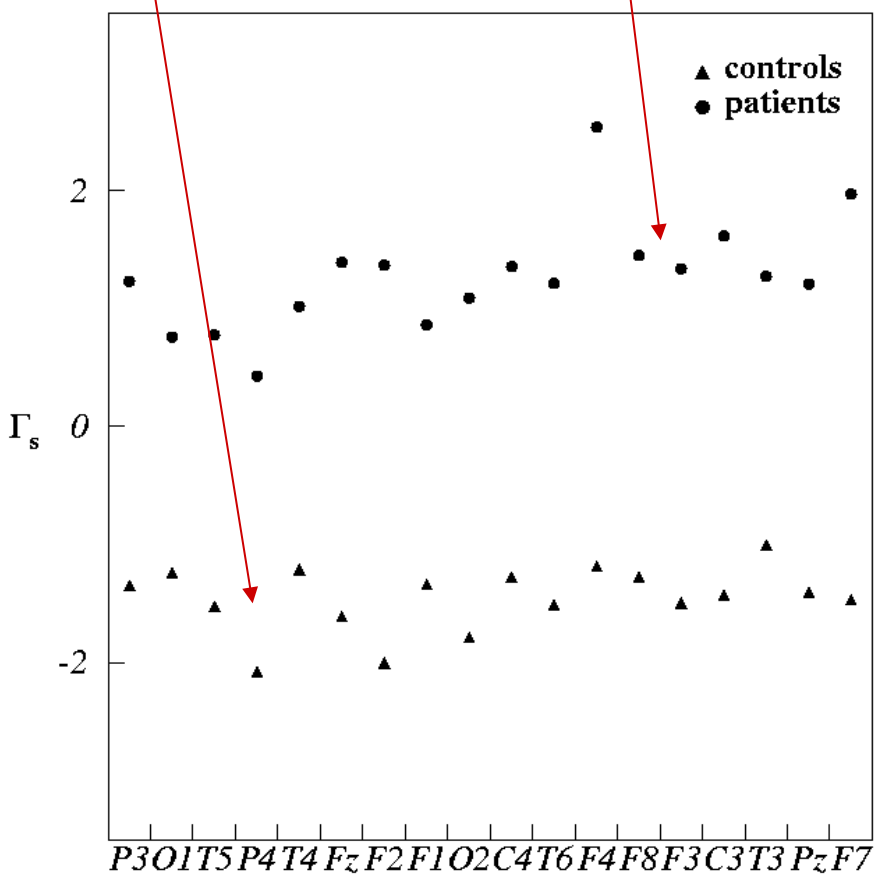

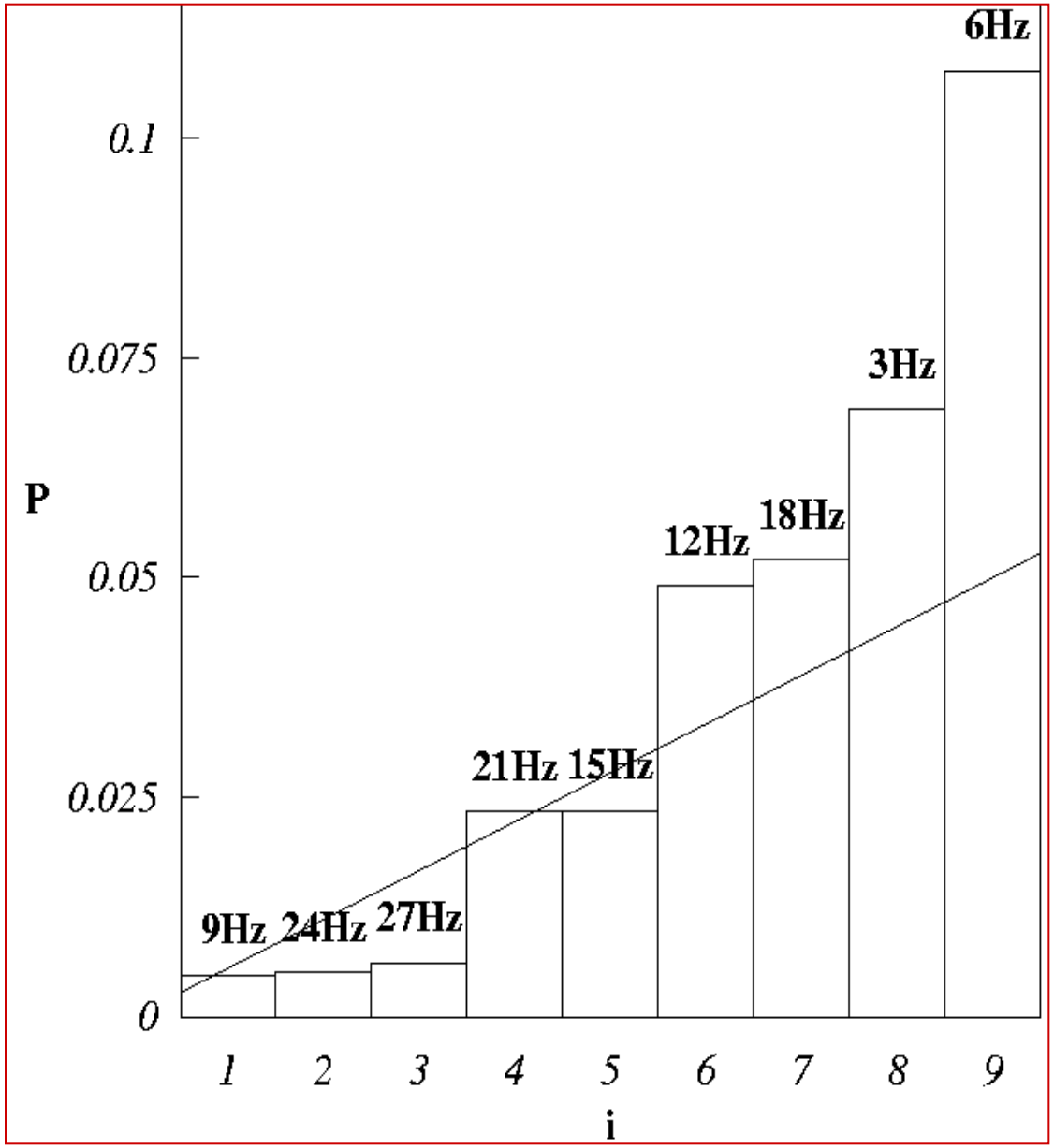

Method of

FALSE DISCOVERY RATE

I: ordering index;
by definition
P(i) increasing

P(i):frequency of ext. stimulus
Data points below straight line meaningful, providing discrimination between controls/patients.

(Good frequencies are 9,24,27 HZ: 9 Hz in α band; 24 Hz and 27 Hz contain subharmonics in α band

Study of synchronization in cardiovascular signals

Tires and Fondazione Maugeri, Montescano (Pavia, Italy)

Systolic blood pressure (SAP) =maximal pressure within the cardiovascular system reached as the heart pumps blood into the arteries. Diastolic pressure (DAP)= minimum in pressure reached while the heart rests and is filled by blood.

The analysis of their fluctuations may provide significant information on the physiology and pathophysiology of the autonomic control of the cardiovascular function. Synchronization of SAP and DAP expected.

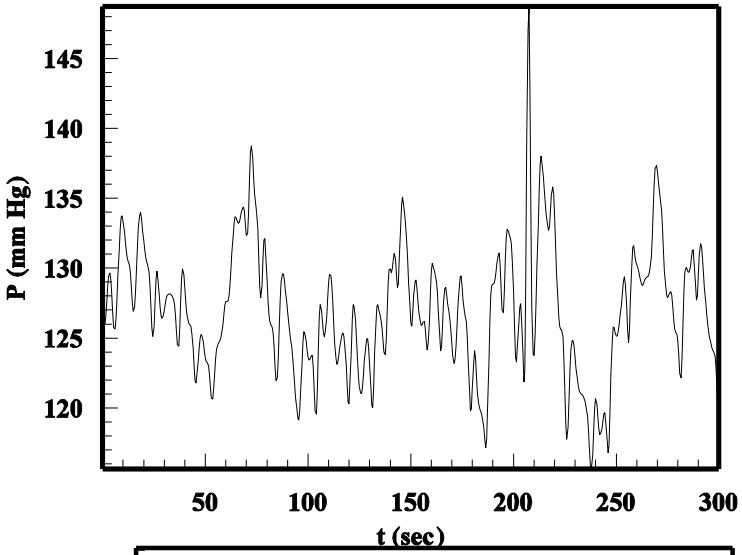

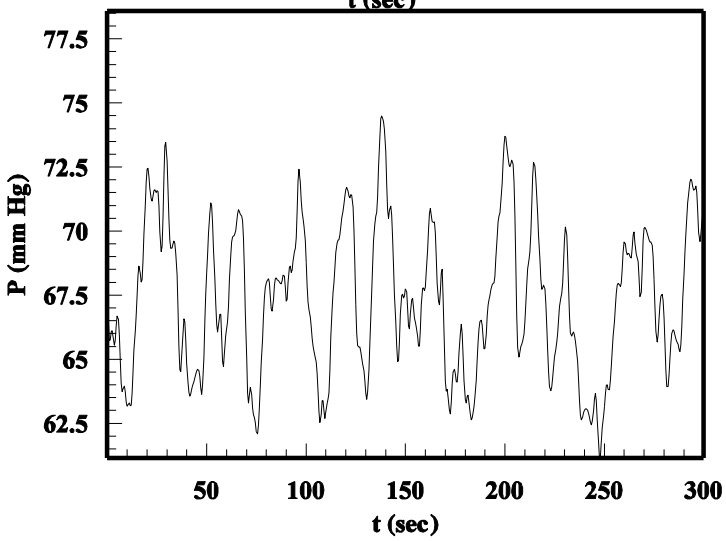

Phase shifts $\delta\theta=\theta_D-\theta_S$ for 47 subjects, filtered in VLF band (here diastolic anticipates) and HF band (here systolic anticipates).

A significant phase delay was found between the two time series by examining data collected in the laboratory for the assessment of Autonomic Nervous Sytem, S. Maugeri Foundation, Scientific Institute of Montescano, Italy. When examined in the Very Low Frequency (VLF) band and in the high frequency (HF) band, the phase shift between DAP and SAP was found positive in VLF band and negative in the HF band.

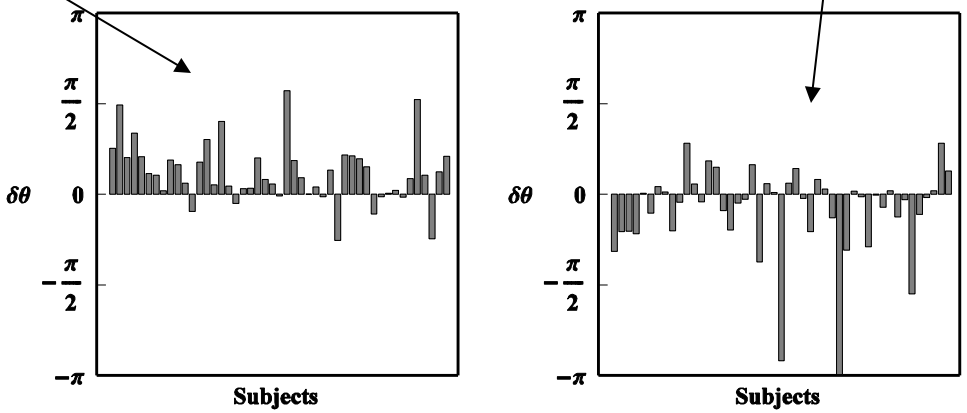

Phases extracted by the Hilbert transform (analytic signal)

$$y(t) = \frac{1}{\pi} P.V. \int_{-\infty}^{+\infty} \frac{x(\tau)}{t-\tau} d\tau$$

Analytic signal $z(t) = x(t) + iy(t) = A(t)e^{i\phi(t)}$

A mechanism based on the Kuramoto model (L.Angelini et al. Phys.Rev. E (2004)

WINFREE model

$$\dot{\theta}_i(t) = \omega_i + \frac{1}{N} \sum_{j=1}^{N} \kappa \, P(\theta_j) \, R(\theta_i)$$

describes a set of $N \gg 1$ coupled non linear oscillators, with coupling constant proportional to κ.

$\theta_i(t)$ phase of the $i-$th oscillator; $\{\omega_i\}$ set of natural frequencies taken randomly from a distribution $g(\omega)$.

$g(\omega) = 1/2\gamma$ for $\gamma \in [\omega_0 - \gamma, \omega_0 + \gamma]$

$P(\theta_j) = 1 + \cos\theta_j$: influence function of the $j-$th oscillator;

$R(\theta_i) = -\sin\theta_i$: sensitivity (response) function of the $i-$th oscillator.

Soluzione grafica (I: piccolo N)

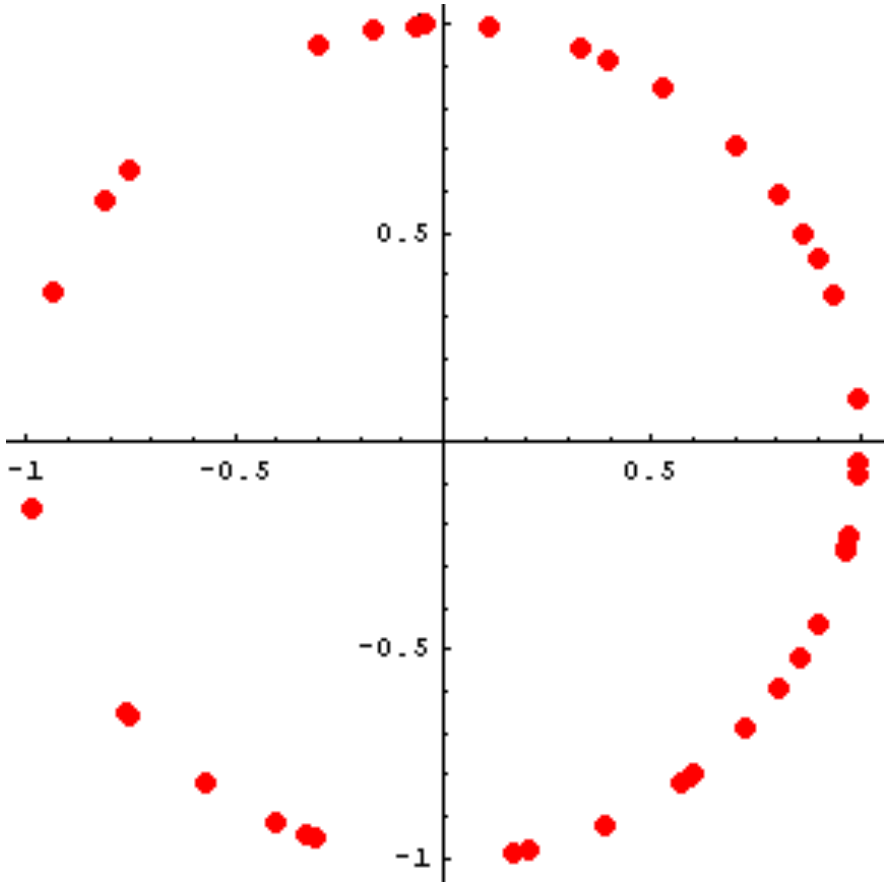

Soluzione grafica (II: N maggiore)

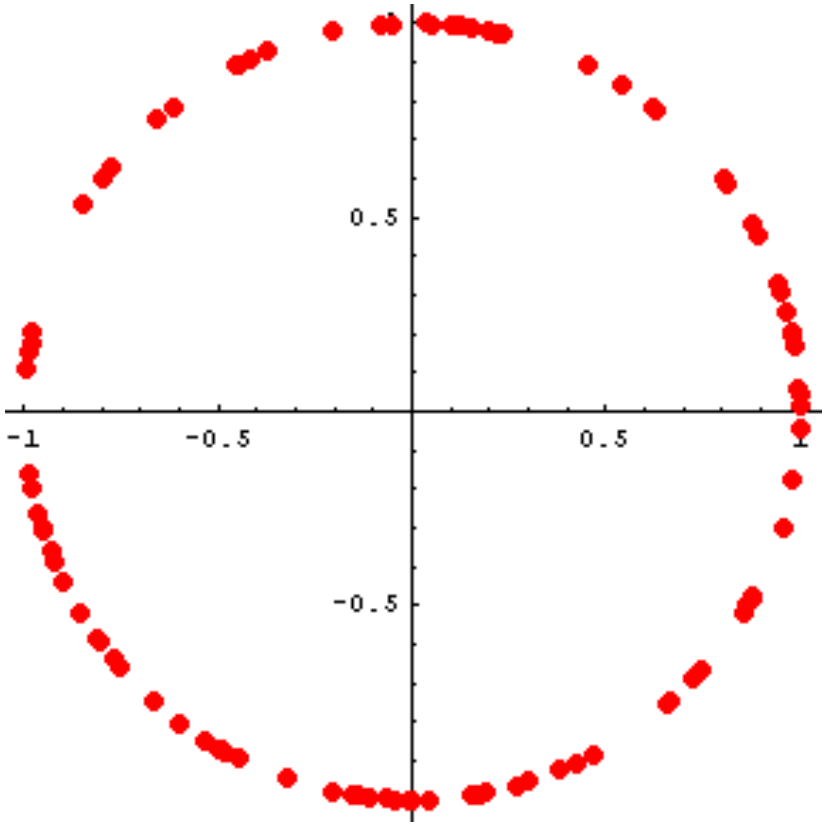

Ringraziamenti: F. Giannuzzi, M.Pellicoro

$$v(\theta, t, \omega) = \omega - \sigma(t) \sin\theta$$

$$\sigma(t) = \kappa \int_0^{2\pi} \int_{1-\gamma}^{1+\gamma} (1 + \cos\theta)\, p\,(\theta, t, \omega)\, g(\omega) d\omega d\theta$$

$p\,(\theta, t, \omega)$ = density of oscillators. At large t after a temporal averaging

$$v = \omega - \frac{1}{T} \int_t^{t+T} dt\, \sigma(t) \sin\theta(t)$$

Considering variations in ω:

$$0 = \delta\omega - \frac{1}{T} \int_t^{t+T} dt\, \sigma(t)\, \delta\theta(t) \cos\theta(t)$$

$\delta\theta(t)$ is time-independent for t large enough:

$$\begin{aligned} \delta\omega &= \frac{\kappa\delta\theta}{T} \int_t^{t+T} dt \int d\omega\, g(\omega) \int_0^{2\pi} d\hat{\theta}\, (1 + \cos\hat{\theta}) \times \\ &\times \; p(\hat{\theta}, t, \omega)\, \cos\theta(t) = \frac{\kappa\lambda}{2} \delta\theta \end{aligned} \qquad (2)$$

where $$\frac{4\gamma^2}{\kappa^2} = \lambda \sin^2\left(\frac{2\gamma}{\kappa\lambda}\right)$$

The slope δθ/δω in the Winfree model. On the left: δθ/δω as a function of κ for two values of ω_0 and γ=0.1. On the right: δθ/δω as a function of γ for two values of ω_0 and κ=0.45. The curves are independent of ω_0.

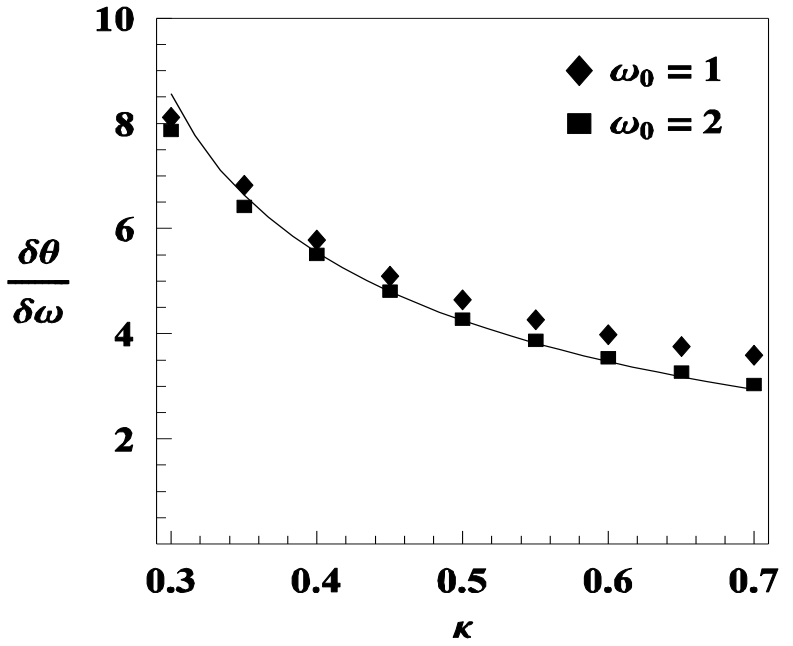

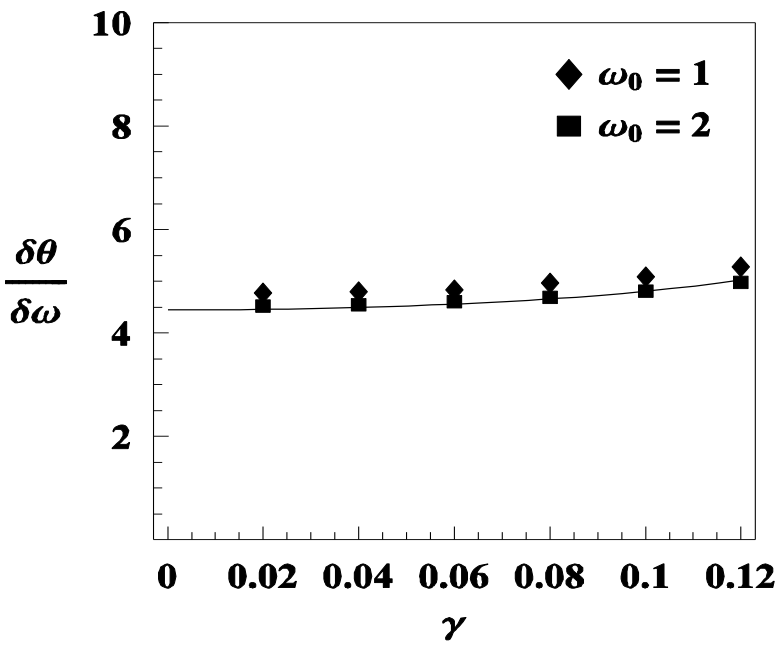

On the left : the rotation number $\rho=\lim_t \theta(t)$ plotted versus ω for $\gamma=0.10$ and $\kappa=$ 0.35, 0.45, 0.65 (from top to bottom). The picture shows the synchronization of the oscillators at large times. On the right: $\delta\theta = \theta_j - \theta_i$ versus $\delta\omega= \omega_j - \omega_i$ for the same values of γ and κ (larger slopes correspond to higher values of κ). This picture shows that phase shifts and differencies of frequencies are linearly related.

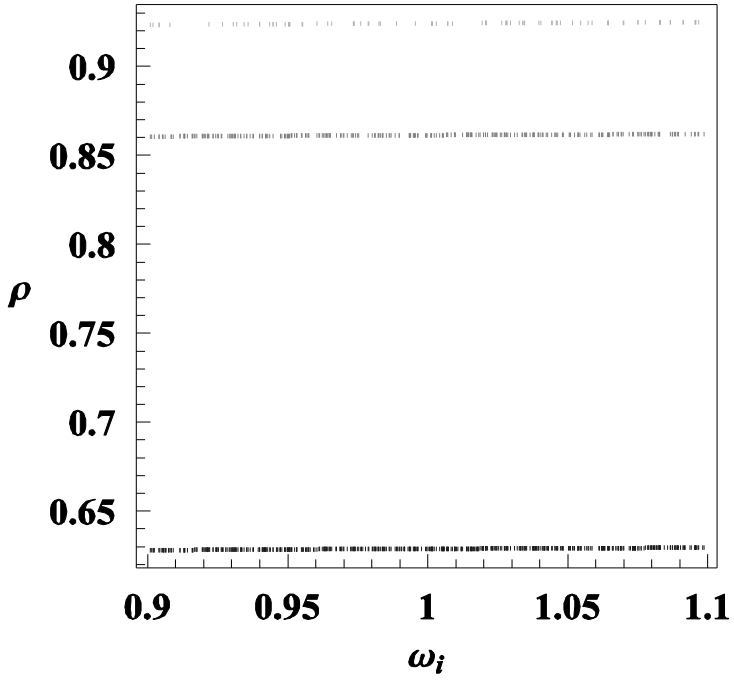

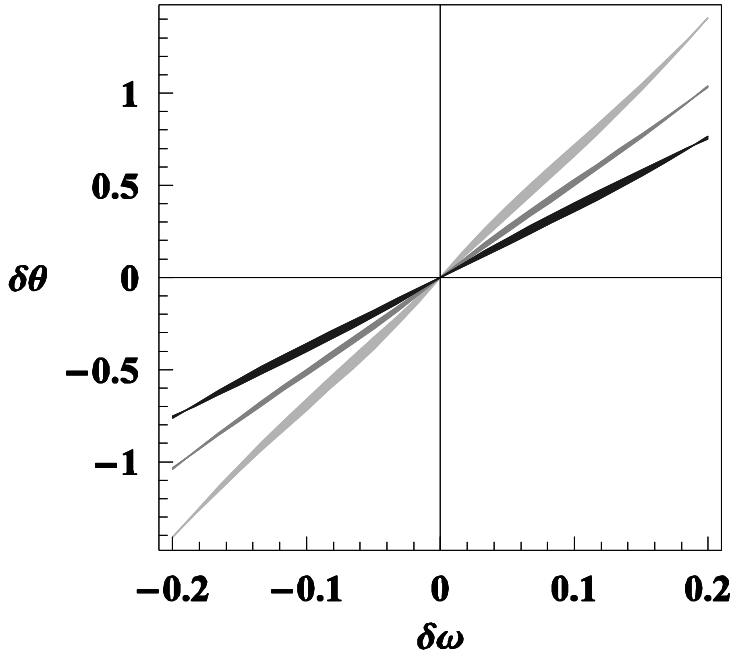

A possible mechanism based on synchronous oscillators

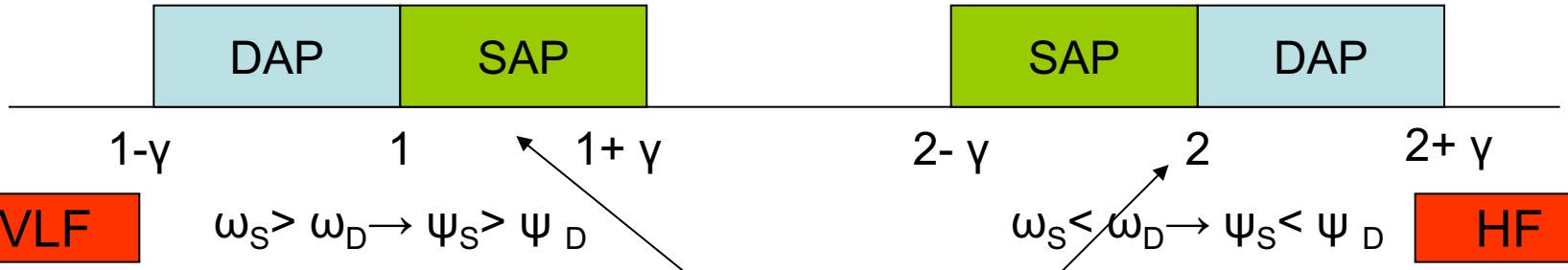

We assume periodic phenomena result from many interacting elementary Winfree oscillators. In the VLF band those responsible for diastolic pressure have ω smaller; in the HF band the opposite occurs

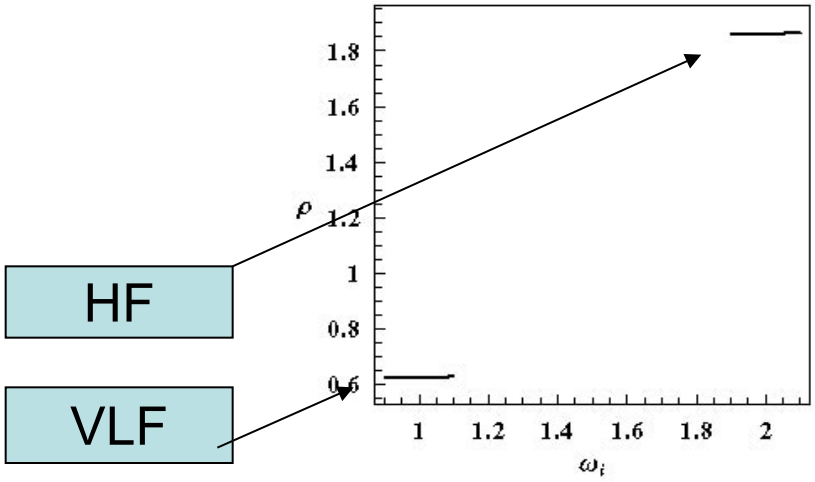

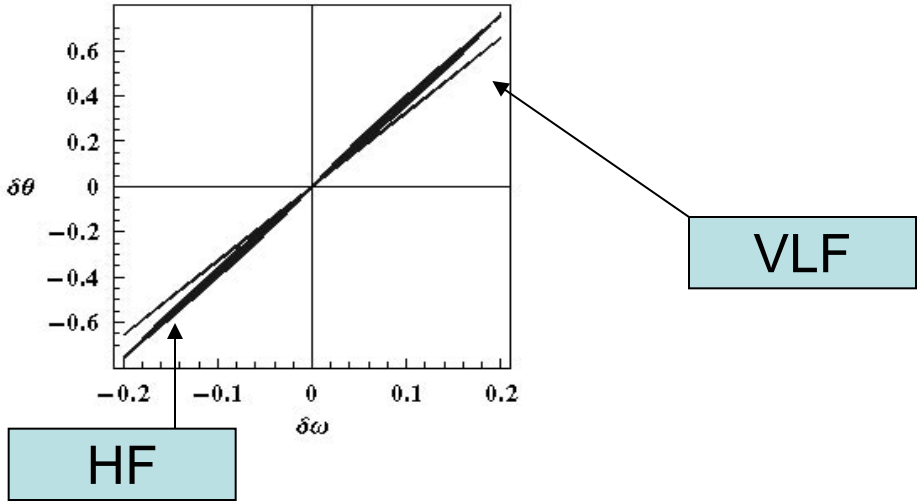

In VLF $\delta\omega>0$ implies $\delta\theta>0$, therefore diastolic pressure anticipates

KURAMOTO model

The Kuramoto model is based on the set of equations ($i = 1, ...N$)

$$\dot{\theta}_i(t) = \omega_i + \frac{\kappa}{N} \sum_{j=1}^{N} \sin(\theta_i - \theta_j)$$

Results similar to the Winfree model:

$$\delta\omega = \kappa\lambda\,\delta\theta$$

λ given by

$$\frac{2\gamma^2}{\kappa^2} = \lambda\left(1 - \cos\frac{2\gamma}{\kappa\lambda}\right)$$

The slope δθ/δω in the Kuramoto model. On the left: δθ/δω as a function of κ for two values of ω_0 and γ=0.1. On the right: δθ/δω as a function of γ for two values of ω_0 and κ=0.45.

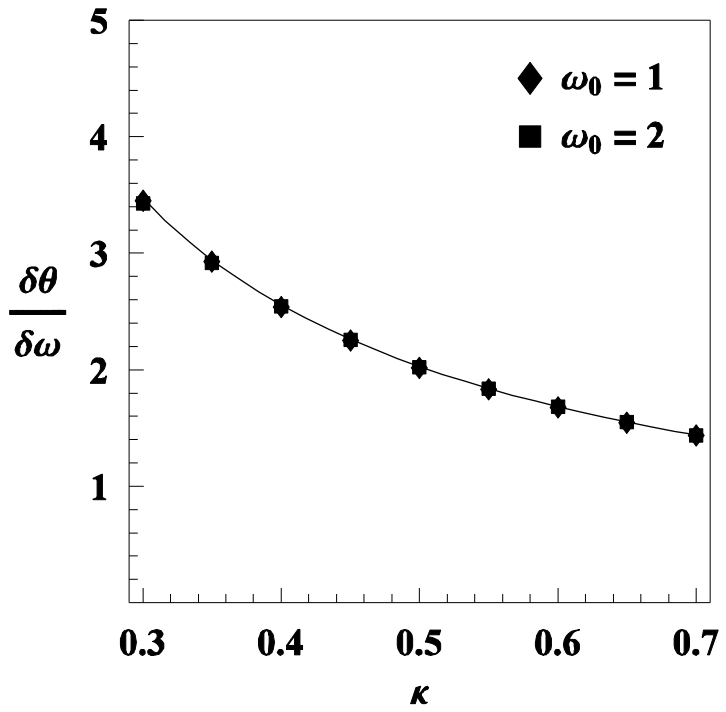

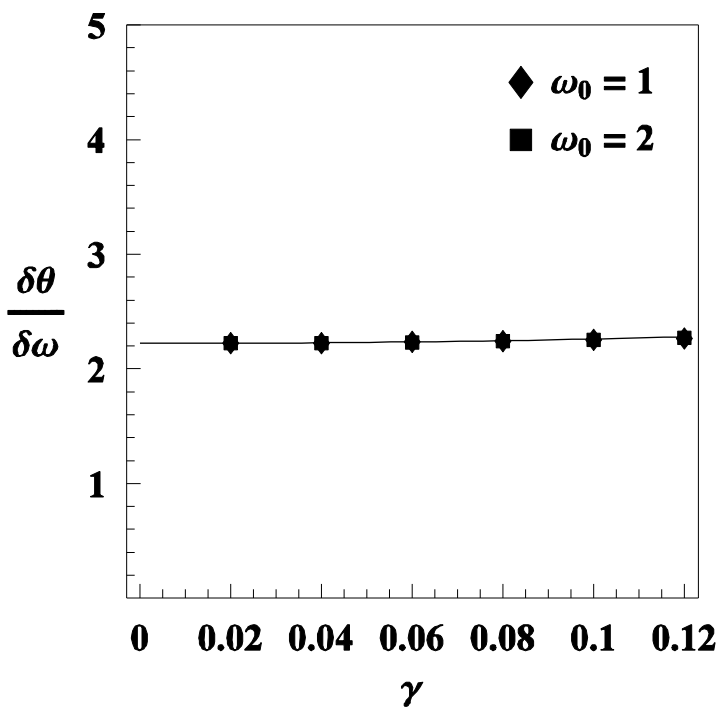

TIRES
Innovative Technologies for Signal Detection and Processing

Research Center of Excellence of Italian Ministry of Education

University of Bari, Italy

- About 30 researchers + PhD+post-doc of the University of Bari
- Physicists (50%) medical faculty (40%) Chemistry Dept. (10%)
- Main activities:

  New detectors for environmental-biomedical applications (L. Torsi, M. De Palma)

  Pattern recognition, modelling and data analysis, mainly biomedical (R.Bellotti, M. DeTomaso, A. Federici, L. Nitti, S. Stramaglia,)

  Recently: protein and genome analysis (G.Lattanzi, F. Volpe)

Conclusions

- Methods of theoretical physics and mathematical physics flexible enough to provide tools for biomedical applications.
- Challenge from data collected by innovative sensors with a wide range of possible applications
- Powerful results from cross disciplinary researches

The MOBIOMAC project (1)

Models of Biological Macromolecules

A two-year project at TIRES (G. Lattanzi) : Marie Curie European Reintegration Grant (EU

3 Objectives

- Objective 1: mechanochemical models

Experimental results from kinesin, a motor protein,

and interpretation by non equilibrium statistical mechanics models.

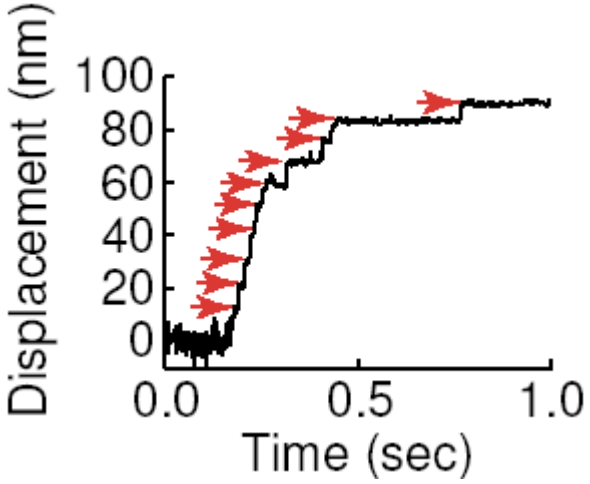

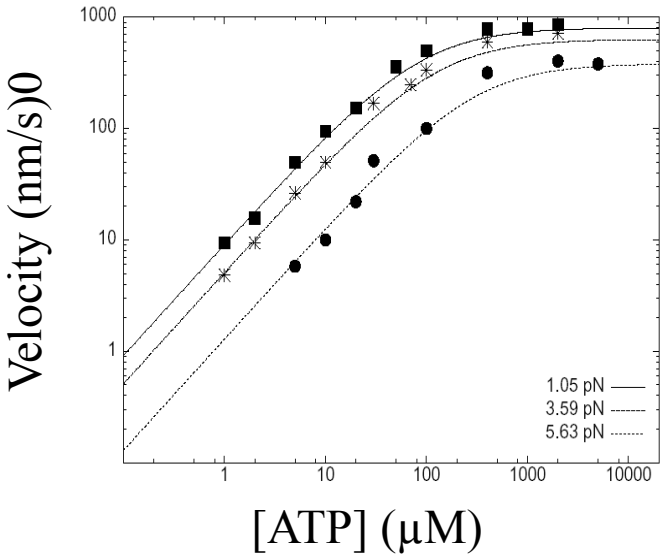

The MOBIOMAC project (2)

- Objective 2: single filament models

Models that describe elastic properties of proteins polymerizing in filaments of known structure, e.g.DNA, microtubules and actin

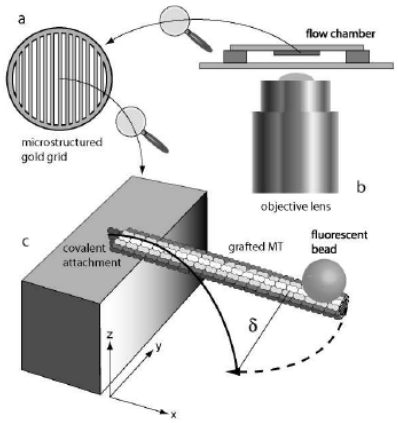

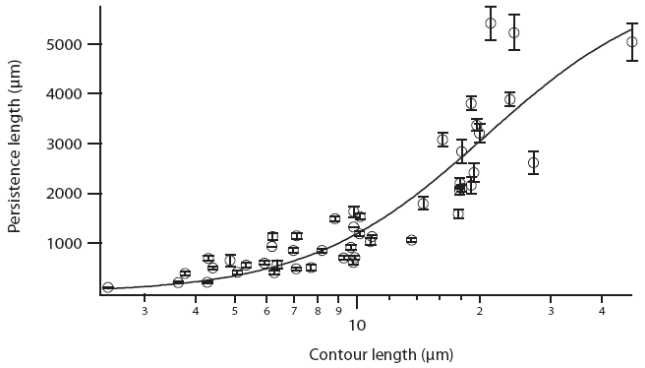

Persistence length for microtubules, Exp in coll. with European Molecular Biology Lab, Heidelberg

- **Objective 3: coarse grained models for proteins: definition, characterization of efficient, reliable computational tools for the analysis of protein structures**

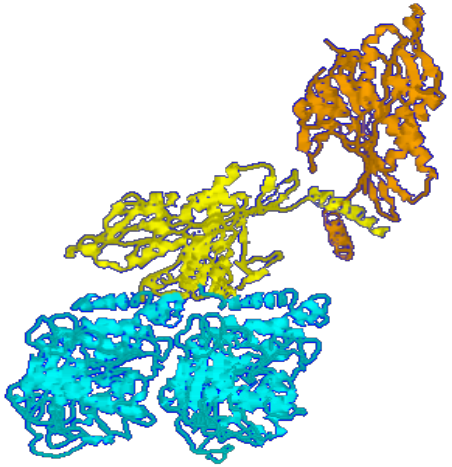

Comparison between "all atoms" molecular dynamics (time scales<100 ns) and coarse grained models able to extend simulated dynamics (in the picture kinesin interacting with tubulin)to time scales of biological relevance (>ms).

Organic thin-film transistors as chemical sensors

Organic thin-film transistor

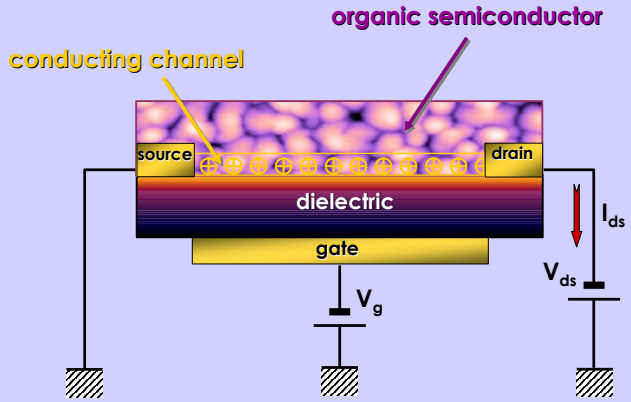

Some common p-type organic semiconductors for thin film transistors

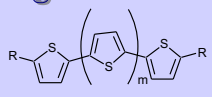

α–Hexathiophene

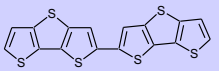

Bis(dithienothiophene)

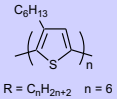

HT-poly(3-alkyl)thiophene

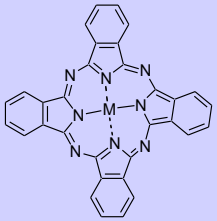

Phtalocyanine

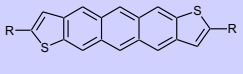

α–ω dialkylanthradithiophene

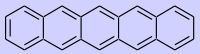

Pentacene

Dimitrakopoulos, C.D.; Malenfant, P.R.L. *Adv. Mater.* **2002**, *14*, 99

L. Torsi and collaborators

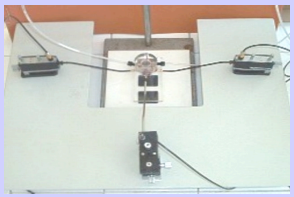

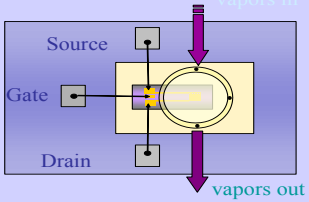

Response repeatability

news

analytical

chemistry Marc 2003

analytical chemistry Marc 2003

ANALYTICAL CURRENTS

Thin-film vapor responses

Whether they are called electronic noses, tongues, or simply sensors, olfactory-mimicking detectors have become a major research arena. L. Torsi, A. Dodabalapur, H. Katz, and co-workers at Lucent Technologies and Università degli Studi di Bari (Italy) provide some framework for this research by investigating the relationship between thin-film molecular structure and morphology and device response. Using 1-pentanol as the analyte, they found that the response is greater when the number of grain boundaries of the film increased. However, the relationship is more complicated with octanonitrile as the analyte.

Various oligothiophene thin films on silicon wafers were studied in this report. For example, thin films of α,ω-dihexyl-α-hexathiophene grown at room temperature were found to consist of small, irregular nanodomains, which probably helped vapors penetrate into the material. Films grown at 120 °C or higher were more regular and lamellar in detail and did not respond as well to pentanol vapors. On the other hand, the response to octanonitrile was independent of film morphology.

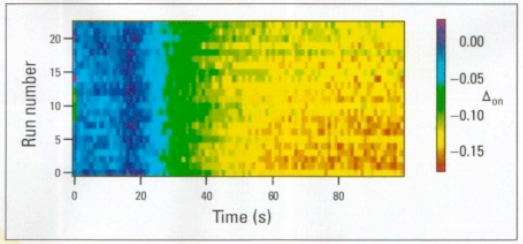

Color-coded changes in the current of a thin-film "electronic nose" sensor to 25 exposures of 1-pentanol.

Other factors investigated included the film's thickness, the chain length in a series of alkyl-substituted hexathiophenes, and the behavior of a short oligomer thiophene. The researchers believe that vapor analyte adsorption is controlled by favorable hydrophobic interactions between the semiconductor and analyte, intercalation to fill defect vacancies, and surface binding. (*J. Phys. Chem. B* **2002,** *106,* 12,563–12,568)

B. Crone et al. *Appl. Phys. Lett*. **78**, 2229 (2001)

L. Torsi et al. *J. of Physical Chemistry B* **106** (48) , 12563-12568 (2002).